polymer papers

Nanophase molecular droplets: individual polystyrene molecules on mica imaged with scanning electron and atomic-force microscopy

R. A. Shelden, L. P. Meier, W. R. Caseri and U. W. Suter*
Eidgenössische Technische Hochschule, Institut für Polymere, CH-8092 Zürich, Switzerland

and R. Hermann and M. Müller
Eidgenössische Technische Hochschule, Laboratorium für Elektronenmikroskopie I, CH-8092 Zürich, Switzerland

and M. Hegner and P. Wagner
Eidgenössische Technische Hochschule, Laboratorium für Biochemie, CH-8092 Zürich, Switzerland
(Received 20 May 1993; revised 12 November 1993)

Scanning electron microscope (SEM) images have been obtained of polystyrene grafted onto mica with ultrahigh specific surface area and sputter coated with 1 nm tungsten. These images show separated 'droplets' of a mean diameter of ca. 30 nm. Comparison of the number and size of these droplets with other experimental data such as weight fraction grafted polymer and molecular weight of the grafted polymer suggests that the droplets observed are nanophases consisting of individual polymer molecules. The droplets have also been imaged using atomic-force microscopy (AFM). The diameters appear larger with AFM than with SEM. This appears to be an artifact of the AFM resulting from the nano-scale needle tip dimensions.

(Keywords: nanophase droplets; polystyrene-grafted mica; scanning electron microscopy)

INTRODUCTION

The development of atomic-force microscopy (AFM) has led to expectations that it will be widely possible to image polymers with molecular resolution. Indeed, there have already been several reports of such images for crystalline polymers[1-7]. Progress in scanning electron microscopy (SEM) has also made possible the imaging of individual biomolecules[8], and the imaging of individual synthetic polymer molecules under suitable conditions therefore also seems possible. However, with the exception of some early work on polystyrene using transmission electron microscopy[9,10], examples of the imaging of individual isolated synthetic polymer molecules by any of these techniques are still not yet in evidence. In this paper, the imaging by SEM and AFM of nanophases consisting of individual polystyrene molecules grafted onto mica via ionic end-groups is reported.

Mica is a popular substrate for surface studies owing to its well defined, flat surface structure[11,12]. Recently the preparation of mica powders with ultrahigh specific surface area has been described[13]. This mica offers a unique opportunity for surface investigations. In particular, the adsorption of a cationic azo initiator, 2,2'-azobisisobutyramidine hydrochloride (AIBA) (*Figure 1*), onto the surface of the mica by ion exchange has been quantitatively investigated[14]. The polymerization of styrene in the presence of this initiator–mica complex was found to result in grafting of polymer to the mica[15]. The grafted polymer was shown to consist of high-molecular-weight chains bound very sparsely to the mica surface by ionic end-groups[15]. The average polymer layer thickness could be calculated to be about 1 nm (for a mica with ca. 4 wt% grafted polymer), but the distribution of this material on the surface, whether it formed a uniform layer or 'islands' or some other structure, was not known. In the present study, these polymer–mica complexes are examined by SEM and AFM.

EXPERIMENTAL

Details of the preparation of the ultrahigh-surface-area mica powders and their surface-area measurement by methylene blue adsorption[13], the preparation of the mica complex by ion exchange with AIBA[14] and the polymerization of styrene with the complex to give polymer-grafted mica[15] have all been previously reported. The high-surface-area mica powders were prepared using as starting material a waste product of mica insulating 'paper' manufacture, the 'fines' that pass through the Fourdrinier screens. The starting material was then further delaminated by treatment with

* To whom correspondence should be addressed

0032-3861/94/08/1571-05

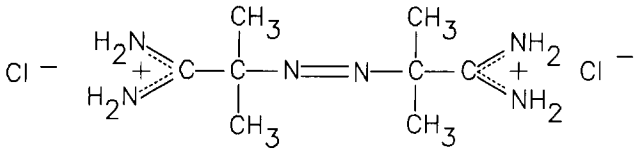

Figure 1 2,2'-Azobisisobutyramidine hydrochloride (AIBA)

concentrated aqueous lithium nitrate for several days at 170°C, giving a mica product with surface areas of about $100\,m^2\,g^{-1}$ as determined with methylene blue adsorption. The individual particles were for the most part smaller than 15 μm in diameter, with an aspect ratio of about 250 as determined with a surface profilometer.

This mica was then dispersed in aqueous solutions of AIBA and left to stand overnight. The suspension was filtered, the mica washed on the filter with water and then methanol, and dried. The amount of AIBA adsorbed (by ion exchange) was determined from the concentration change in the supernatant solution as measured by u.v. spectroscopy and was found to be about 4 $\mu mol\,m^{-2}$ of mica surface.

The polymer-grafted mica was prepared by suspending the AIBA-treated mica in styrene at 60 or 80°C for various periods of time. The resulting solids were then repeatedly extracted with toluene to remove the soluble polymer. Finally, the mica was washed with methanol, dried and analysed by thermal gravimetric analysis (t.g.a.). The toluene-insoluble polymer that remained with the mica could not be removed by tetrahydrofuran (THF) alone, but could be removed by THF containing 1 wt% lithium chloride (presumably by ion exchange). The polymer so dissolved was examined by ^1H n.m.r., g.p.c. and light scattering. The data indicate the polymer to be polystyrene with number-average molecular weight of about 1×10^6.

For SEM, the mica powders were glued to 20 μm thick copper sheet (Goodfellow Metals, Cambridge, UK) with the help of a minute layer of conductive carbon cement (Neubauer Leit C, Münster, Germany). The samples were then sputter coated with 1 nm tungsten[16]. Samples were observed in a Hitachi S-900 in-lens field-emission SEM at 30 kV accelerating voltage (beam diameter < 1 nm)[17]. In some cases, instead of using the conductive carbon cement, the samples were mounted on double-faced transparent plastic tape. The images were basically the same with both methods, but the quality of the images was poorer when the tape was used instead of the conductive carbon because of electrical charging.

The identical tungsten-coated samples, after examination by SEM, were examined by AFM. The AFM measurements were performed under ambient conditions on a commercially available Nanoscope III atomic-force microscope (Digital Inc., Santa Barbara, CA, USA). Scanners were calibrated in all dimensions with the use of the Nanoprobe Silicon Calibration Standard #1 (Si/200 nm period). The known lattice constants were observed by measuring highly oriented pyrolytic graphite (HOPG) and mica; z calibration was confirmed by STM measurement of the step heights on Au(1 1 1). Cantilevers were monocrystalline silicon with integrated silicon tips (Nano Sensors, Wetzlar, Germany); spring constants were in the range 0.08 to 0.17 $N\,m^{-1}$. Image acquisition in the constant-force imaging mode was done in air at room temperature with repulsive forces on the order of 10 nN.

RESULTS AND DISCUSSION

Figure 2 shows an electron micrograph of a sample of polystyrene-grafted mica. For this sample, polymerization was carried out at 80°C for 21 h, and t.g.a. showed a polymer content of 3.8 wt% based on total weight. The micrograph shows 'droplets' distributed on the mica surface. The droplets are not present in electron micrographs of a tungsten-coated control sample of mica that was treated with AIBA and heated in the absence of styrene (*Figure 3*). The distribution of droplet diameters $f(D)$ measured manually from the electron micrograph for the 3.8 wt% sample is shown in *Figure 4*. Droplets smaller than about 10 nm in diameter could not be readily distinguished and may be underrepresented in the count. The average diameter of the droplets counted was ca. 30 nm (about 2 nm of this is tungsten coating). A styrene chain with molecular weight of 1×10^6 forming a hemisphere on the surface with the usual density of polystyrene, ca. $1.04\,g\,cm^{-3}$, would have a diameter of about 18 nm. Thus the observed mean droplet size is greater than, but of the same order of magnitude as, that expected for individual molecules if they formed hemispheres. The difference can be attributed to a number of possible factors: (1) the droplets being spherical segments with contact angles less than 90° rather than hemispheres; (2) overestimation of mean droplet size through underrepresentation of smaller droplets in the count; (3) uncertainty in the estimated average molecular weight of the chains; and (4) a possible lower density for these individual molecules than for bulk polystyrene.

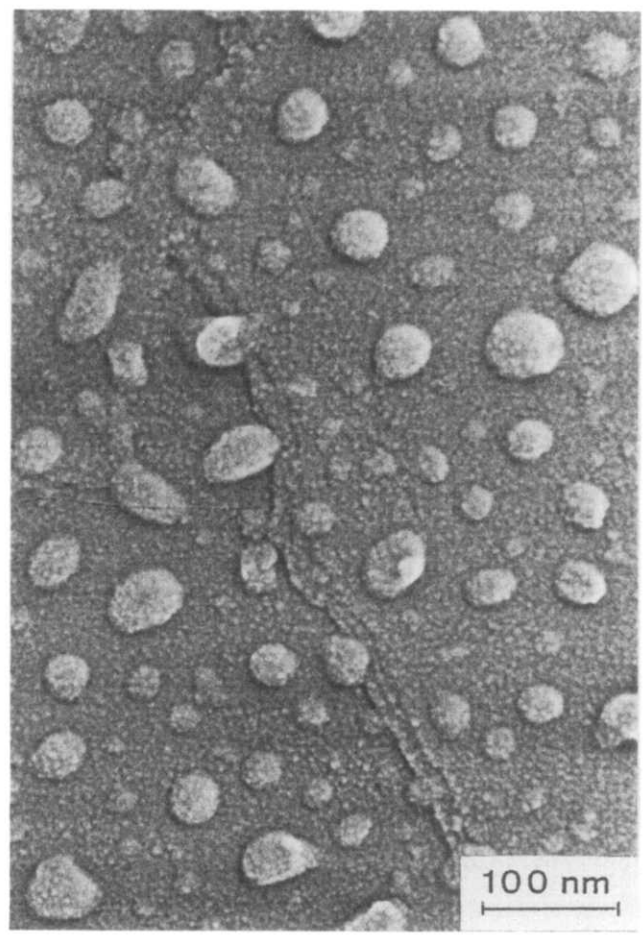

Figure 2 High-resolution SEM micrograph (Hitachi S-900) of polystyrene-grafted mica powder sputter coated with 1 nm tungsten

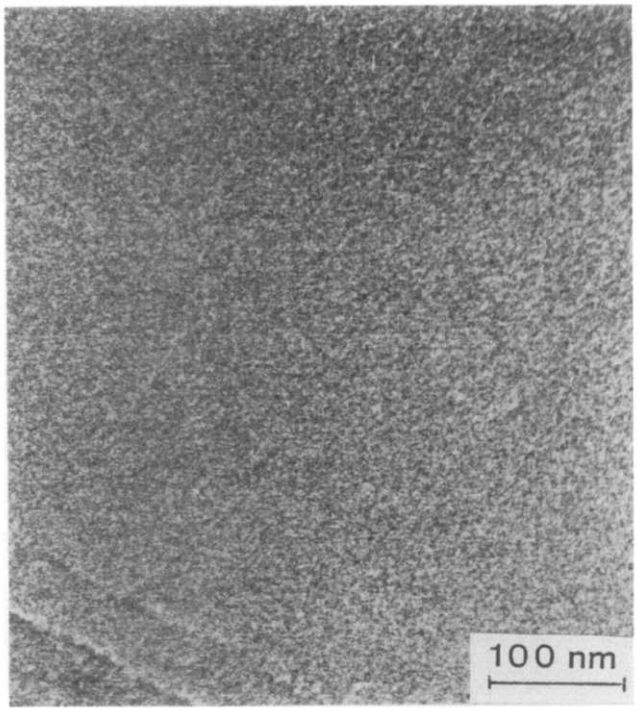

Figure 3 High-resolution SEM micrograph (Hitachi S-900) of AIBA–mica powder (control) sputter coated with 1 nm tungsten

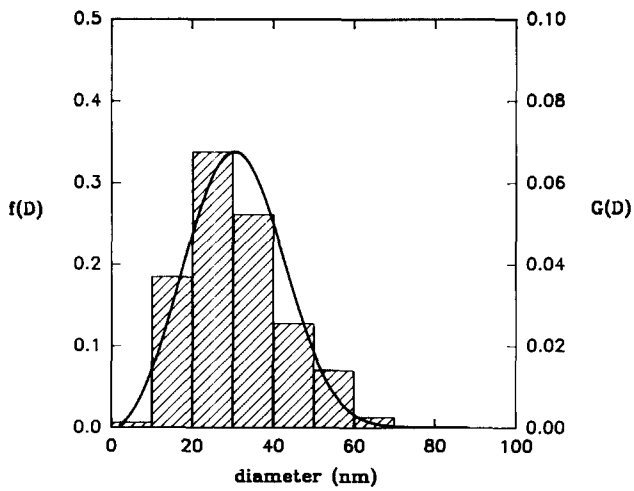

Figure 4 Experimental histogram ($f(D)$) and 'most probable' continuous frequency distribution ($G(D)$) of diameters

If the macromolecules did form individual droplets, would they be spaced far enough apart to be distinguishable? For the mica specific surface area of ca. $100\,m^2\,g^{-1}$, a molecular weight for the polystyrene of 1×10^6 and 3.8 wt% polymer in the product, there would be about one chain end per $4200\,nm^2$ of surface. Since there is about one ion-exchange site per $0.48\,nm^2$ (ref. 15), only about one in 9000 of the ion-exchange sites has chain ends attached. This corresponds to a mean spacing between chain ends of about 65 nm. With a mean diameter per droplet of 20–30 nm, the droplets would be readily distinguishable. Indeed a mean spacing between droplets of about 65 nm seems consistent with that observed in *Figure 2*.

If the droplets are indeed individual molecules, the size distribution of the droplets should reflect the distribution of the degree of polymerization, x. For simplicity, the 'most probable' distribution of diameters was calculated assuming the 'most probable' distribution[18] of chain lengths x (see Appendix for details), and is plotted in *Figure 4* for comparison with the experimental distribution of diameters. Agreement between the two is good.

It will perhaps be noted that the most probable distribution of diameters differs significantly in shape from the most probable distribution of chain lengths. On a linear scale of chain lengths, the fraction of chains with a given chain length decreases monotonically with increasing chain length (see Appendix). In contrast, and perhaps surprisingly, the most probable distribution of diameters shown in *Figure 4* exhibits a maximum as diameter increases. The agreement between theory and observation in *Figure 3* is therefore all the more striking.

Further support for the 'molecular droplet' hypothesis comes from the mass of polymer on the mica surface. It was estimated from *Figure 2* that there are about 3×10^{14} droplets/m^2 of mica surface. If each droplet contained one chain of molecular weight 1×10^6, each would weigh about 1.7×10^{-18} g. With a mica specific surface area of $100\,m^2\,g^{-1}$, the polymer would amount to about 5.0 wt% of the polymer–mica complex. This is close to the 3.8 wt% polymer found by t.g.a. Equivalently, the 3×10^{14} droplets/m^2 of mica surface estimated from *Figure 2* is equivalent to one droplet per $3300\,nm^2$. This is close to the value of one chain end per $4200\,nm^2$ previously discussed.

SEM examination of a grafted mica with 1.2 wt% polymer showed droplets with the same average diameter as found for the 3.8 wt% sample, and the distribution of diameters was very similar in both cases. As a result, one would expect the number of droplets per unit area for the 1.2 wt% sample to be about one-third that of the 3.8 wt% sample (the ratio of the polymer weight fractions shown by t.g.a.). In fact, the SEM images for the 1.2 wt% sample showed a number of droplets per unit area about 45% of the number for the 3.8 wt% sample. The agreement appears to be within experimental error (t.g.a., counting of the droplets, variations from one location to another, etc.).

The same tungsten-coated samples used for electron microscopy were also examined by AFM. Sample images at two different magnifications are shown in *Figures 5* and *6*. A profile is also displayed in *Figure 5* (note that the vertical and horizontal scales in the profile are not identical). As with SEM, droplets were observed and the images are qualitatively similar. The number of droplets per unit area is similar to that found with SEM. However, the droplets appear to be larger in the AFM images (about twice as large) than in the SEM images and therefore closer together than with SEM. We believe this to be due to an artifact of the AFM measurements, resulting from the nano-scale needle tip dimensions. There are previous reports in the literature of very similar anomalous size measurements with scanning tunnelling microscopy (STM)[19]. These were attributed to 'tip–sample convolution artifacts' in that work, and it was predicted that the exaggeration of diameters would be even greater with AFM because of the larger needle diameters used at that time in AFM[19]. The AFM needle tip diameters used in the present work are reported by the manufacturer to be under 20 nm. If they were just under 20 nm, then, for a hemispherical droplet of the same diameter, geometric considerations indicate that the AFM image would show (i) almost twice the true

diameter, (ii) a contact angle about two-thirds the true value, and (iii) the correct height for droplets spaced sufficiently apart. In the AFM images, the droplet heights appear to be one-quarter to one-third of the diameters and the contact angles roughly 35° to 60°. Possibly some of the differences between the AFM and STM images

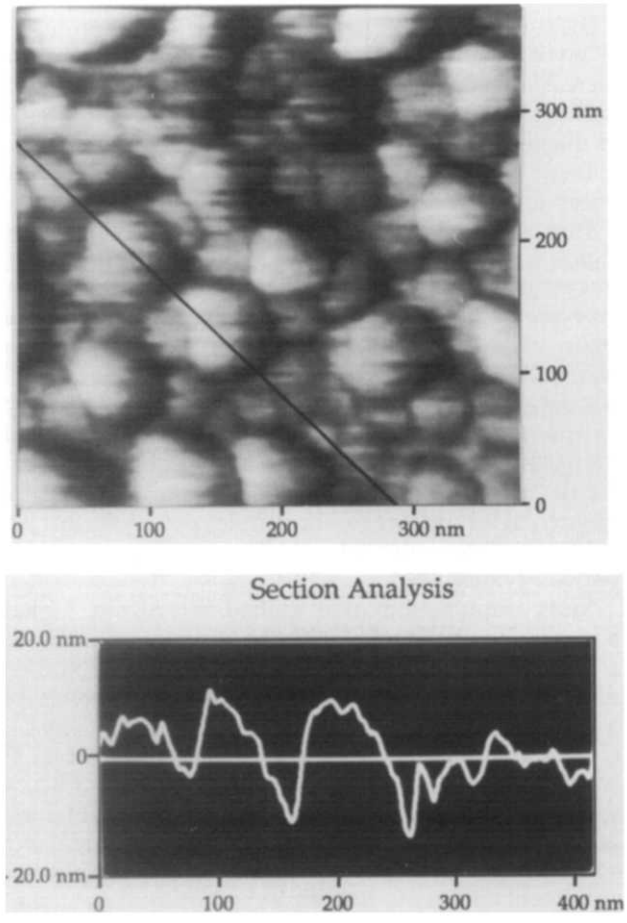

Figure 5 AFM micrograph and profile (Nanoscope model III) of polystyrene-grafted mica powder sputter coated with 1 nm tungsten. Size: 387 nm × 387 nm. Location of profile section is indicated by line on micrograph

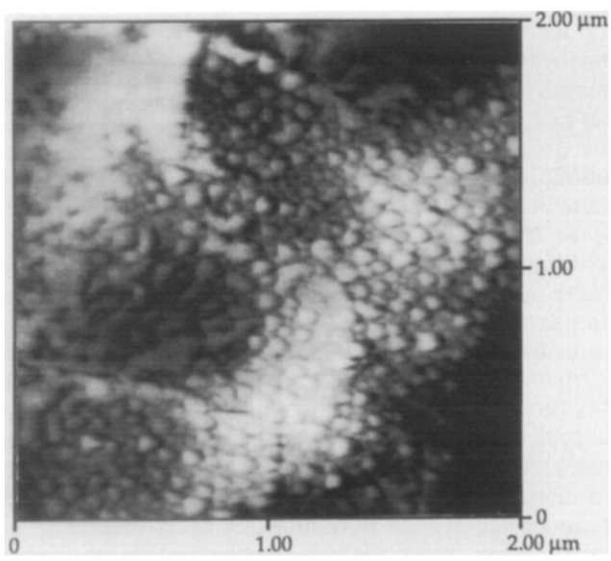

Figure 6 AFM micrograph (Nanoscope model III) of polystyrene-grafted mica powder sputter coated with 1 nm tungsten. Size: 2 μm × 2 μm

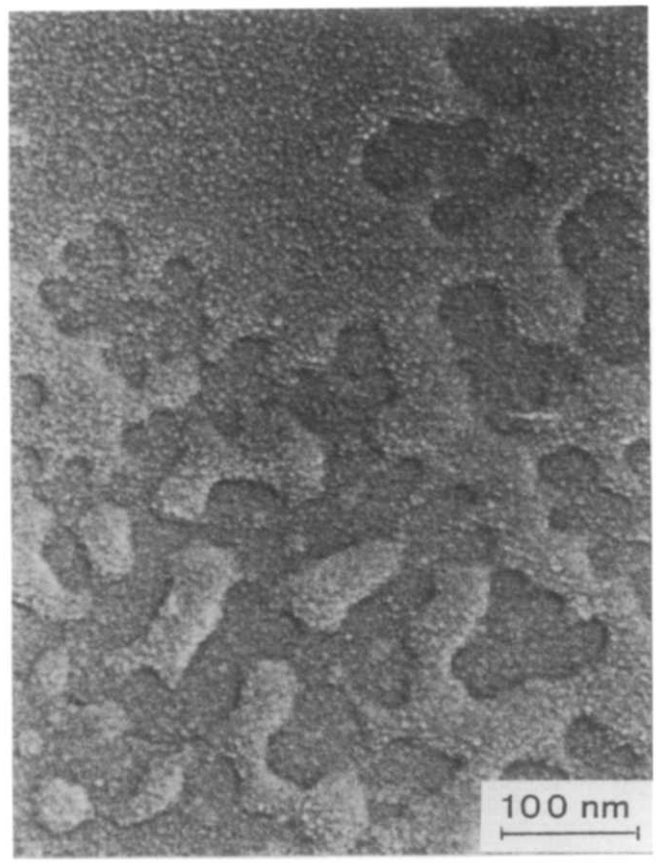

Figure 7 High-resolution SEM micrograph (Hitachi S-900) of polystyrene-grafted mica powder sputter coated with 1 nm tungsten

stem simply from differences in the sample areas examined. However, taken as a whole, the AFM results and the SEM results appear to be consistent if the droplets are roughly hemispherical with diameters as shown by SEM and heights as shown by AFM.

Some of the SEM and AFM images exhibited noteworthy features other than droplets. In particular, in *Figure 7* is shown an electron micrograph of what appears to be a transition region between a droplet structure and a film structure. Probably, either films or droplets can result depending upon local conditions. *Figures 2* and *3* also render the edges of silicate layers. These were also observed in some of the AFM images.

Finally, we would like to comment on the appearance of the molecular droplets as compared with macroscopic multi-molecule droplets on surfaces. The molecular droplets look remarkably like macroscopic droplets of liquid on a poorly wetted surface. Some nearby droplets even appear to have 'run together'. Much useful information has been obtained with macroscopic surface wetting studies, and it might be that the study of bound molecular droplets will provide new and additional insights. It is hardly likely that exactly the same wetting behaviour will be observed with bound nano-scale molecular droplets as is observed with macroscopic droplets having diameters five to six orders of magnitude larger. For example, when a molecular droplet spreads on a surface under the influence of chain-surface interactions, elastic forces arise that tend to limit the extension of the droplet. The elastic forces result from the geometric constraints of the droplet shape on the constituent chain's conformation, elastic forces that do not arise for macroscopic droplets.

CONCLUSION

Taken as a whole, we feel the evidence suggests that the droplets observed with SEM and AFM are nanophases consisting of individual polystyrene molecules attached by their chain ends to the mica surface. The diameters of the droplets appear to be correctly imaged by SEM but exaggerated by AFM because of a needle tip artifact. The height of the droplets appears to be correctly estimated by AFM.

ACKNOWLEDGEMENTS

We gratefully acknowledge financial support for this work through the (Swiss) Kommission zur Förderung der wissenschaftlichen Forschung (KWF) and the (Swiss) Schwerpunktprogramm Werkstofforschung (SPP-WF) as well as stimulating discussions with several members of the Research Divisions of Isola, Breitenbach (Switzerland) and Asea Brown Boveri, Baden (Switzerland). We also thank Professor G. Semenza for kind support and fruitful discussions in the area of AFM.

REFERENCES

1 Marti, O., Ribi, H. O., Drake, B., Albrecht, T. R., Quate, C. F. and Hansma, P. K. *Science* 1988, **239**, 50
2 Magonov, S. N., Quarnström, K., Elings, V. and Cantow, H.-J. *Polym. Bull.* 1991, **25**, 689
3 Hansma, H., Motamedi, F., Smith, P., Hansma, P. and Wittman, J. C. *Polymer* 1992, **33**, 647
4 Stocker, W., Bickmann, B., Magonov, S. N., Cantow, H.-J., Lotz, B., Wittman, J. C. and Möller, M. *Ultramicroscopy* 1992, **42–44**, 1141
5 Snétivy, D. and Vansco, G. J. *Macromolecules* 1992, **25**, 3320
6 Snétivy, D., Rutledge, G. C. and Vansco, G. J. *J. Am. Chem. Soc. Polym. Prepr.* 1992, **33**, 786
7 Snétivy, D., Guillet, J. E. and Vansco, G. J. *Polymer* 1993, **34**, 429
8 Hermann, R. and Müller, M. *Arch. Histol. Cytol.* 1992, **55**, Suppl., 17
9 Richardson, M. J. *Proc. Royal Soc. A* 1964, **279**, 50
10 Barnikol, Von I., Barnikol, W. K. R., Beck, A., Campagnari-Terbojević, Jovanović, N. and Schultz, G. V. *Makromol. Chem.* 1970, **137**, 111; Barnikol, Von I., Barnikol, W. K. R., Jovanović, N. and Schultz, G. V. *Makromol. Chem.* 1970, **137**, 123
11 Guzonas, D., Boils, D. and Hair, M. L. *Macromolecules* 1991, **24**, 3383
12 Guzonas, D. A., Hair, M. L. and Tripp, C. P. *ACS Symp. Ser.* 1991, **447**, 237
13 Caseri, W. R., Shelden, R. A. and Suter, U. W. *Colloid Polym. Sci.* 1992, **270**, 392
14 Shelden, R. A., Caseri, W. R. and Suter, U. W. *J. Colloid. Interface Sci.* 1993, accepted for publication
15 Caseri, W. R., Shelden, R. A. and Suter, U. W. in 'Polymer–Solid Interfaces' (Eds. J. J. Pireaux, P. Bertrand and J. L. Brédas), Institute of Physics, Bristol, 1992, pp. 121–32
16 Hermann, R. and Müller, M. J. *Electron Microsc. Techn.* 1991, **18** (4), 440
17 Nagatani, T., Saito, S. and Yamada, M. *Scanning Microsc.* 1987, **1** (3), 901
18 Flory, P. J. 'Principles of Polymer Chemistry', Cornell University Press, Ithaca, NY, 1953, Ch. VIII, pp. 317–46
19 Blackford, B. L., Jericho, M. H. and Mulhern, P. J. *Scanning Microsc.* 1991, **5** (4), 907

APPENDIX

In the following, we consider the distribution of droplet diameters $G(D)$ under the three assumptions: (i) there is one molecule per droplet; (ii) x, the degree of polymerization (hereafter simply the chain 'length'), is proportional to the cube of the droplet diameter D (as for hemispheres or similar spherical segments); and (iii) the distribution of x is the 'most probable' distribution[18].

From assumption (iii), $N(x)$, the (number) fraction of chains with chain length x, is given by the normalized distribution[18]:

$$N(x)=(1-p)p^{x-1} \qquad \sum_1^x N(x)=1 \tag{A1}$$

where p is a probability parameter ($0 \leqslant p < 1$) and the number-average degree of polymerization is[18]:

$$\overline{x_n}=1/(1-p) \tag{A2}$$

For high polymers ($p \to 1$), the discrete function in equation (A1), valid for integer values of x, can be approximated by a normalized continuous function of x:

$$F(x)=-(\ln p)p^x \qquad \int_0^\infty F(x)\,dx=1 \tag{A3}$$

where $F(x)\,dx$ is the fraction of chains with x values in the interval dx. From assumptions (i) and (ii):

$$x=kD^3 \tag{A4}$$

where k is a constant, and:

$$dx/dD=3kD^2 \tag{A5}$$

Let $G(D)$ represent the distribution of diameters, i.e. $G(D)\,dD$ is the fraction of chain droplets with diameters in the interval dD. $G(D)$ is related to $F(x)$ in that the fraction of chains with x values in the interval dx is the same as the fraction of chain droplets with diameters in the *corresponding* interval dD:

$$G(D)\,dD=F(x)\,dx \tag{A6}$$

Combining equations (A4) to (A6) gives:

$$G(D)=-3k(\ln p)D^2p^{kD^3} \qquad \int_0^\infty G(D)\,dD=1 \tag{A7}$$

To prepare a plot of $G(D)$ *versus* D, the value of k (as well as p) is required. The value for k can be found from the requirement:

$$\overline{x_n}=k\overline{D^3} \tag{A8}$$

The value of $\overline{D^3}$ was found from the SEM images to be 42 140 nm^3. Thus from equation (A8), for $\overline{x_n}=10\,000$ (molecular weight 1.04×10^6), $k=0.2373$ nm^{-3}. It can be shown that, for a polystyrene hemisphere with $x=10\,000$ and density 1.04 g cm^{-3}, D^3 would equal 6423 nm^3, and k would have the value of 1.56. That $\overline{D^3}$ estimated from SEM is larger, and the k value correspondingly smaller, than that calculated for the hemisphere is probably due to the same factors that account for the difference between droplet diameter estimated from SEM and droplet diameter calculated for a hemisphere. These are discussed in the text. For example, if the true mean diameter were 16 nm rather than 30 nm, or if the contact angle were 22° rather than 90°, the difference in the k values would be accounted for.

The value of p can be found from equation (A2). For $\overline{x_n}=10\,000$, $p=0.9999$. A plot of $G(D)$ *versus* D, from equation (A8), for $p=0.9999$ and $k=0.2373$ nm^{-3}, is shown in *Figure 4* in the text.

The mean diameter can be calculated from the function $G(D)$ using the equation:

$$\overline{D}=\int_0^\infty DG(D)\,dD \tag{A9}$$

This integral was evaluated by numerical integration and the resulting value of $\overline{D}$ was found to be 31.1 nm, in good agreement with the measured value of 30.2 nm.